

Supporting Information

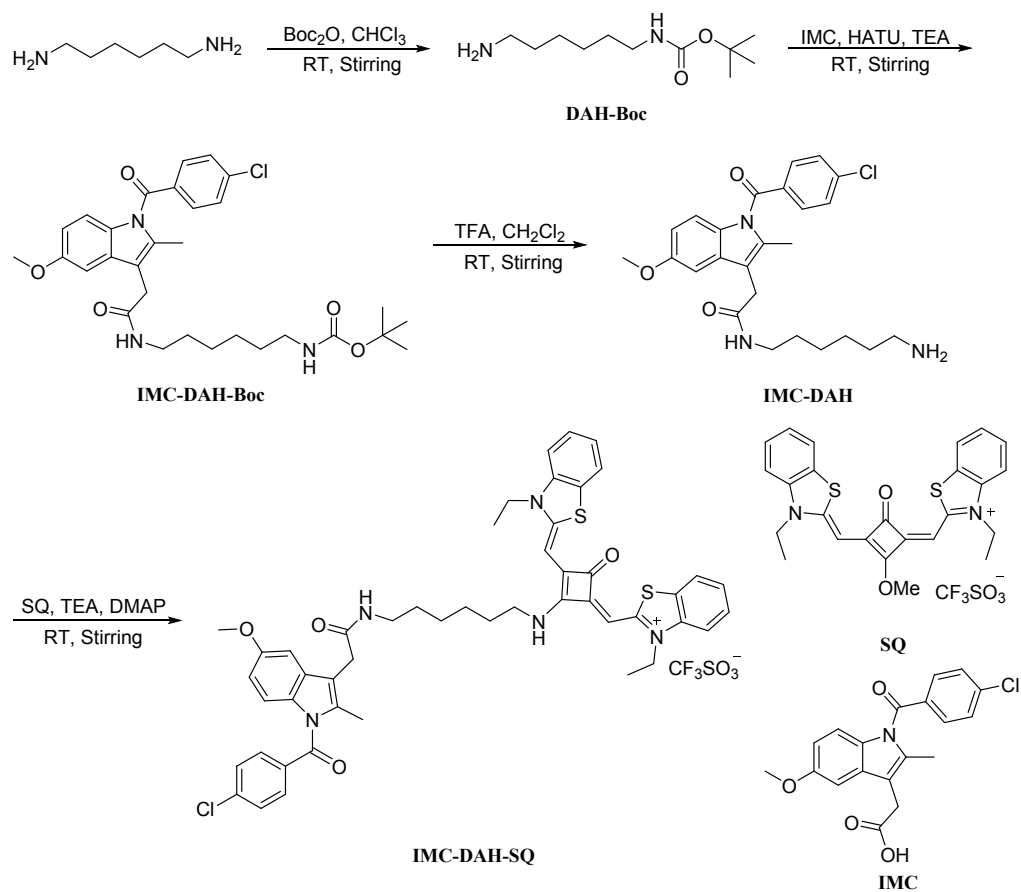
for

Nanoscale photosensitizer with tumor-selective turn-on fluorescence and activatable photodynamic therapy treatment for COX-2 overexpressed cancer cells

Lan Wang, Yuhuan Zhang, Ying Han, Qi Zhang, Zhenfu Wen, Hongjuan Li, Shiguo
Sun, Xin Chen and Yongqian Xu*

Shaanxi Key Laboratory of Natural Products & Chemical Biology, College of
Chemistry & Pharmacy, Northwest A&F University, Yangling, Shaanxi, 712100, P.R.
China

*Corresponding author (E-mail address: xuyq@nwsuaf.edu.cn)



Scheme S1. The synthetic route of **IMC-DAH-SQ**.

Table S1. Spectroscopic properties of **IMC-DAH-SQ** in different solvents.

Solvent	λ_{abs} (nm)	λ_{em} (nm)	Φ
EtOH	663	686	0.10
DMSO	673	696	0.11
CH_2Cl_2	668	689	0.18
Dioxane	667	690	0.38
EtOAc	667	688	0.20
H_2O	607/654	671	0.03

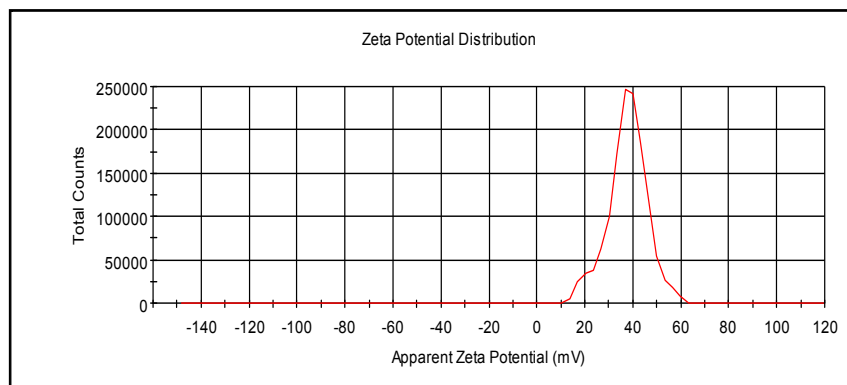


Fig. S1. The Zeta Potential Distribution of **IMC-DAH-SQ** in aqueous solution.

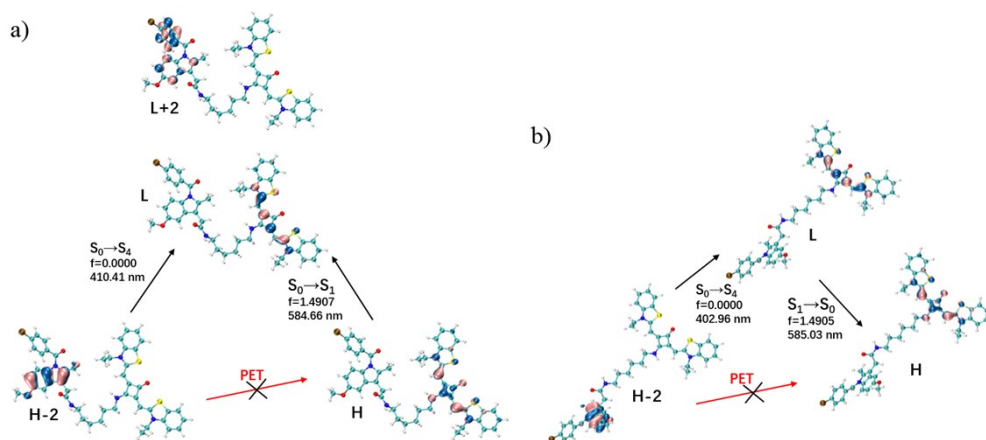


Fig. S2. Structural optimization and the frontier molecular orbital of folded (a) and (b) unfolded **IMC-DAH-SQ** calculated with time-dependent DFT using Gaussian 09.

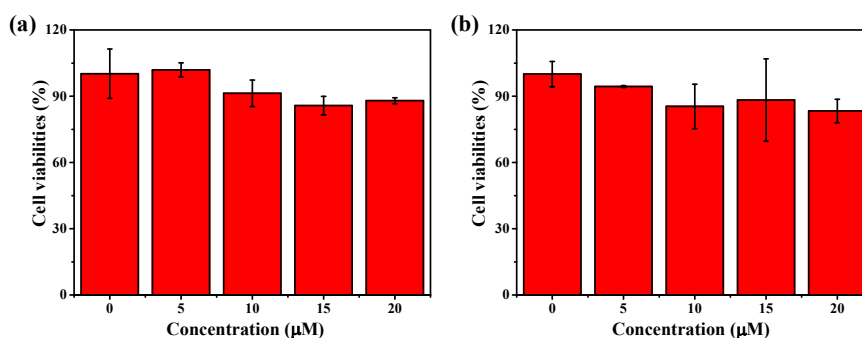


Fig. S3. Cell viability of **IMC-DAH-SQ** estimated by MTT assay. a) HepG-2 cells and b) HL7702 were incubated with different concentrations of **IMC-DAH-SQ** (0-20 μM) for 24 h.

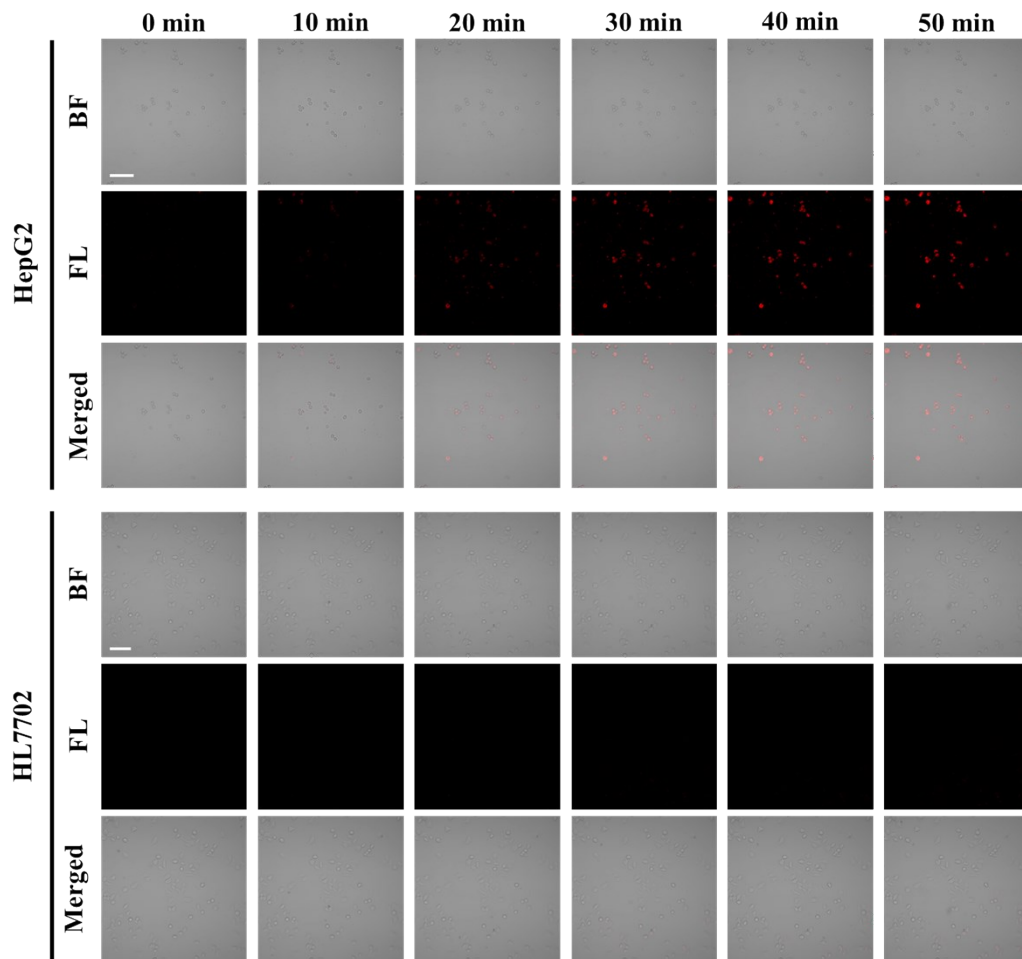


Fig. S4. Real-time fluorescence images of IMC-DAH-SQ in HepG2 and HL7702; Scale bar: 100 μm .

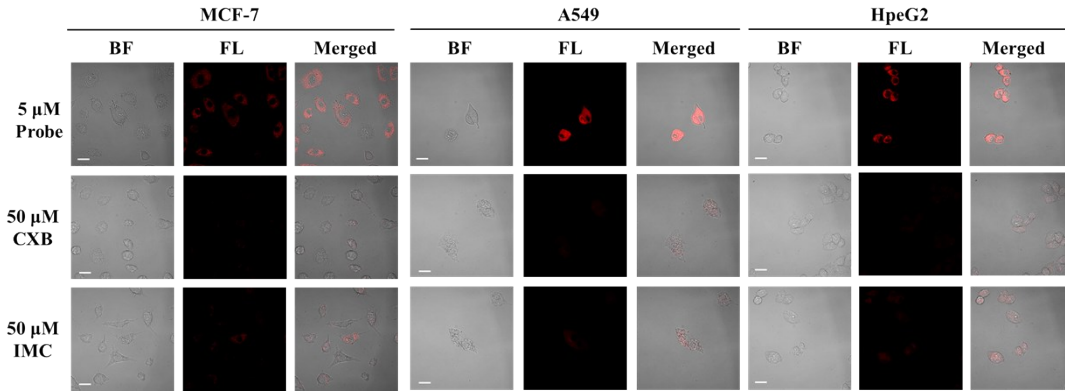


Fig. S5. The pre-incubation inhibitor experiment of COX-2. Cancer cell lines were pretreatment with COX-2 specific inhibitors (IMC and CXB, 50 μ M) for 16 h, then incubated with **IMC-DAH-SQ** (5 μ M) for another 30 min. Scar bar: 20 μ m.

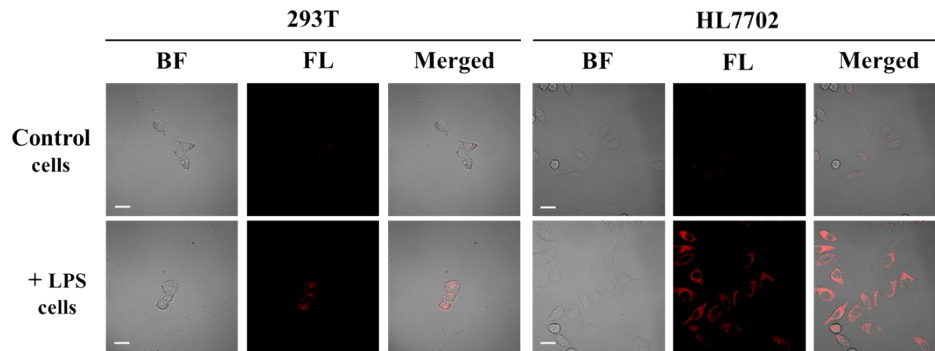


Fig. S6. The experiment of LPS up-regulates COX-2 levels in normal cell lines (293T and HL7702). The normal cells were processed with nanoprobe **IMC-DAH-SQ** for 0.5 h after incubated with LPS for 12 h. Scale bar: 20 μ m.

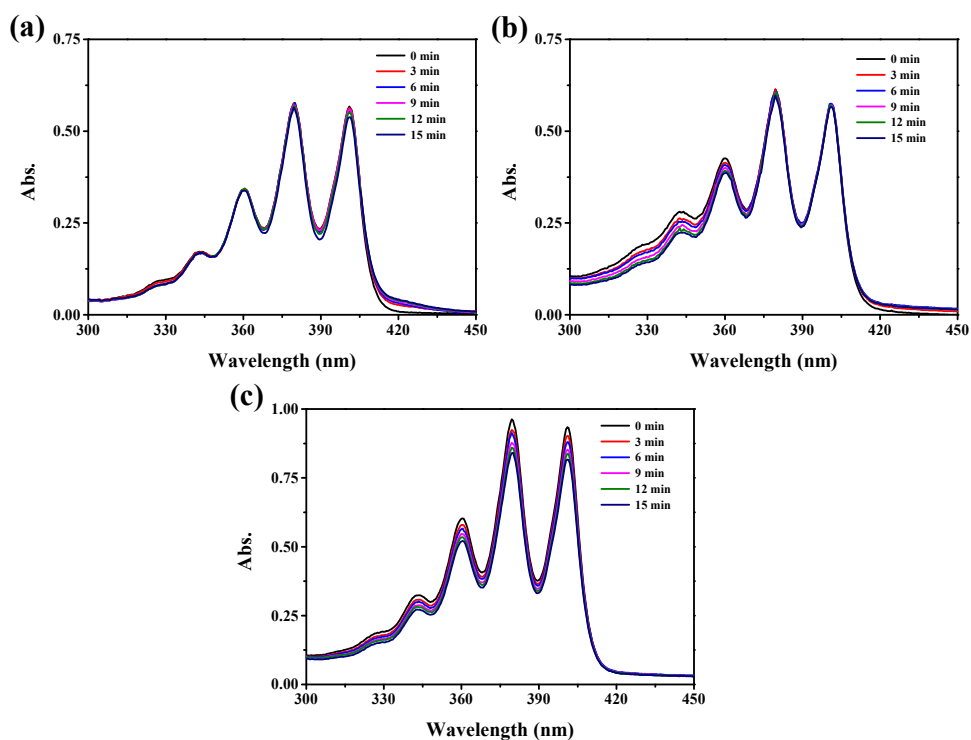


Fig. S7. UV-Vis spectra of 50 μM ABDA upon mixing with (a) 5 μM SQ, (b) 5 μM IMC-DAH-SQ, (c) 5 μM IMC-DAH-SQ+COX-2 followed by irradiation at a power density of 25 mW/cm^2 for different times.

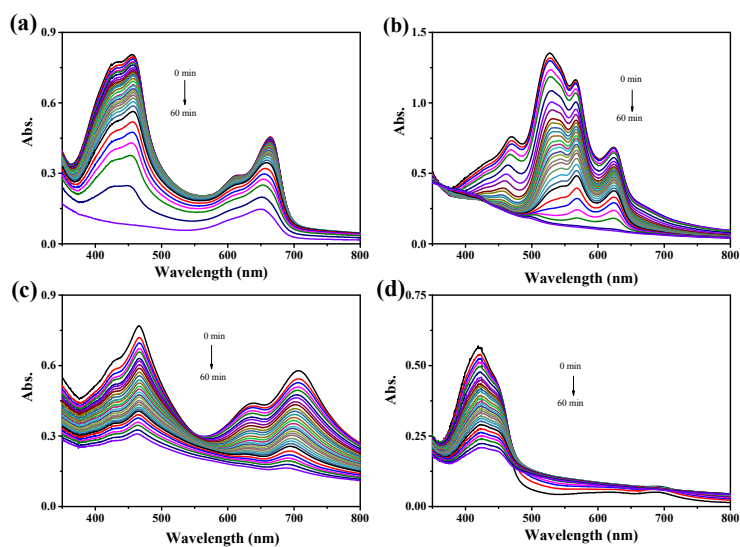


Fig. S8. UV-Vis absorption spectra change of DPBF in the presence of MB (a), SQ (b), IMC-DAH-SQ (c) and IMC-DAH-SQ with COX-2 (d) upon irradiation by laser at 630 nm for different time

in PBS (pH=7.4).

Table S2. ROS quantum yield of MB, SQ, **IMC-DAH-SQ** and **IMC-DAH-SQ+COX-2**.

Substance	Φ
MB	0.52
SQ	0.00665
IMC-DAH-SQ	0.00567
IMC-DAH-SQ+COX-2	0.0352

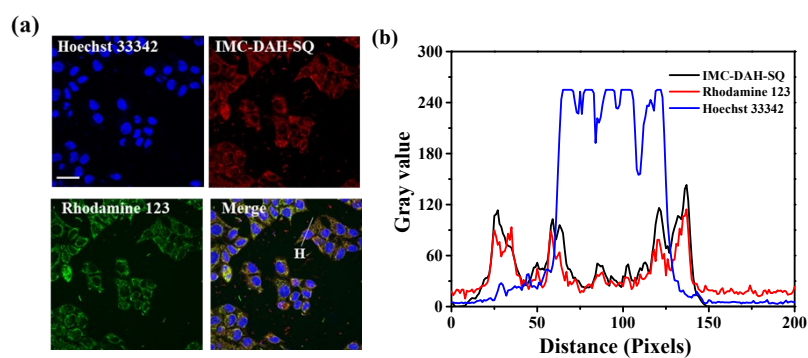


Fig. S9. (a) Co-localization fluorescence images of 5 μ M **IMC-DAH-SQ** and 5 μ M Rhodamine 123 in HepG2 cancer cells. The excitation wavelength is 635 nm and scanning range is 645-700 nm, the excitation wavelength for Rhodamine 123 is 488 nm and scanning range is 500-540 nm; (b) Plot profile of beeline H in merge channel of **IMC-DAH-SQ** and Rhodamine 123. Scale bar: 20 μ m.

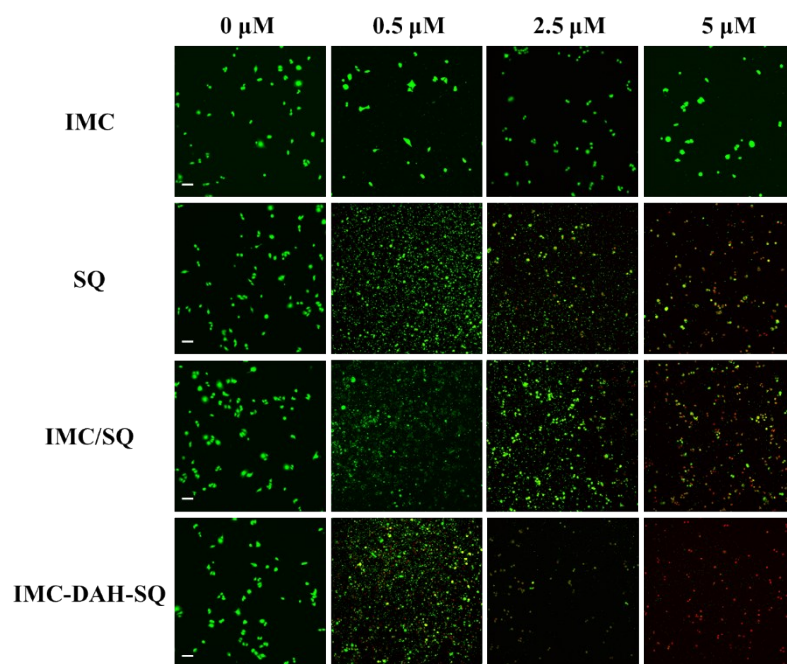


Fig. S10. The confocal imaging of Calcein-AM/PI with different concentration IMC, SQ, IMC/SQ mixture and **IMC-DAH-SQ** upon near-infrared light irradiation (25 mW cm^{-2} , 12.5 min, 630 nm). Scale bar: $100 \mu\text{m}$.

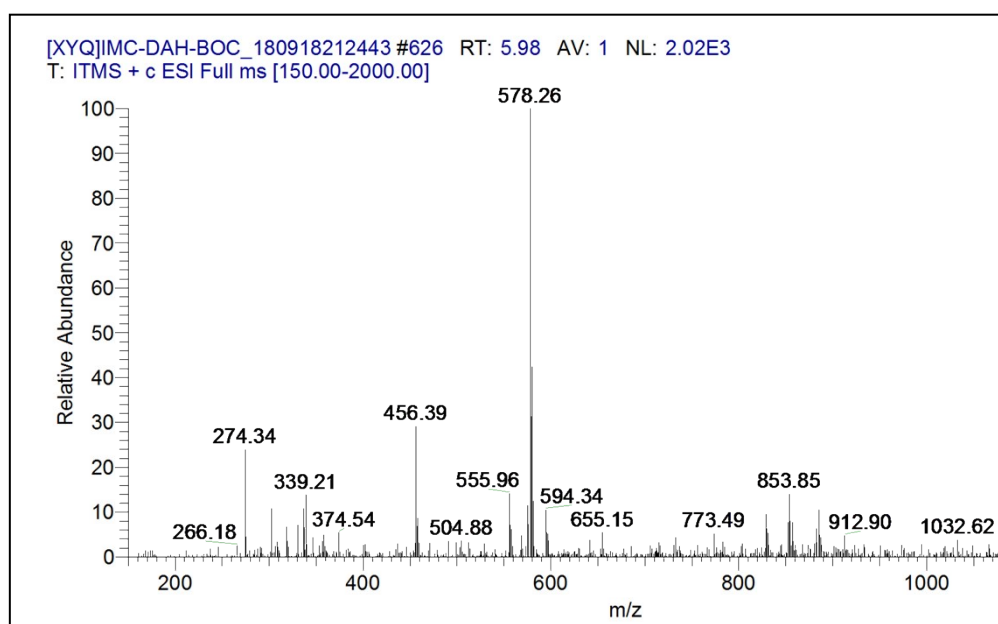


Fig. S11. ESI mass spectrum of IMC-DAH-Boc.

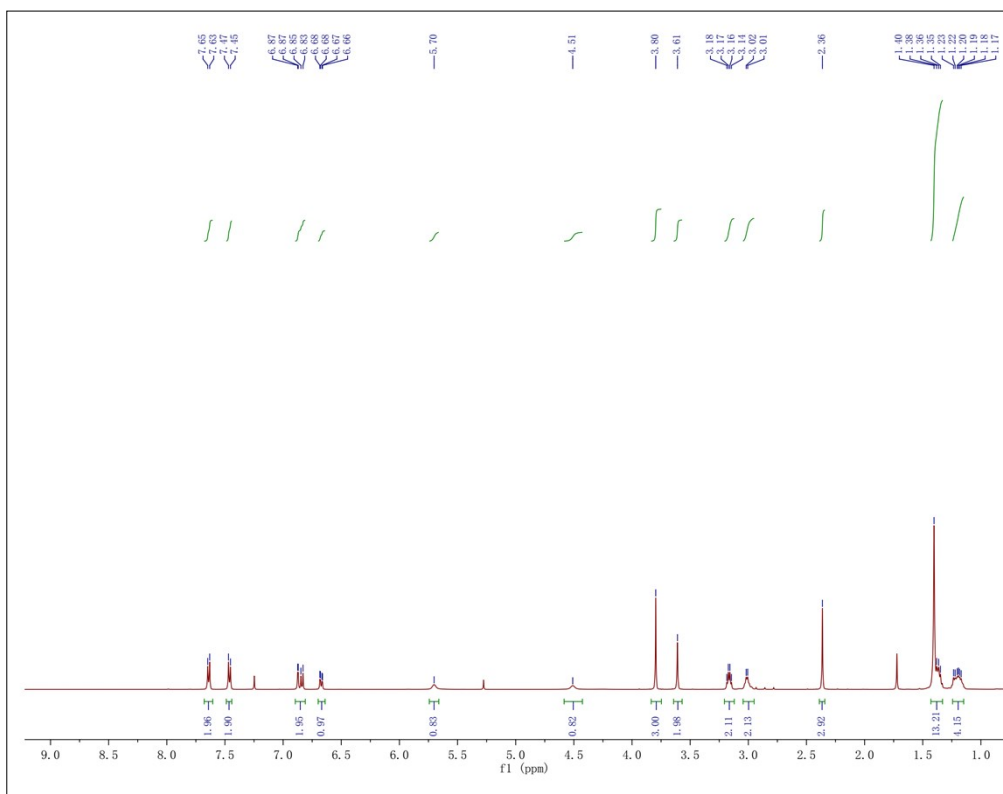


Fig. S12. ^1H NMR spectrum of IMC-DAH-Boc in CDCl_3 solvent.

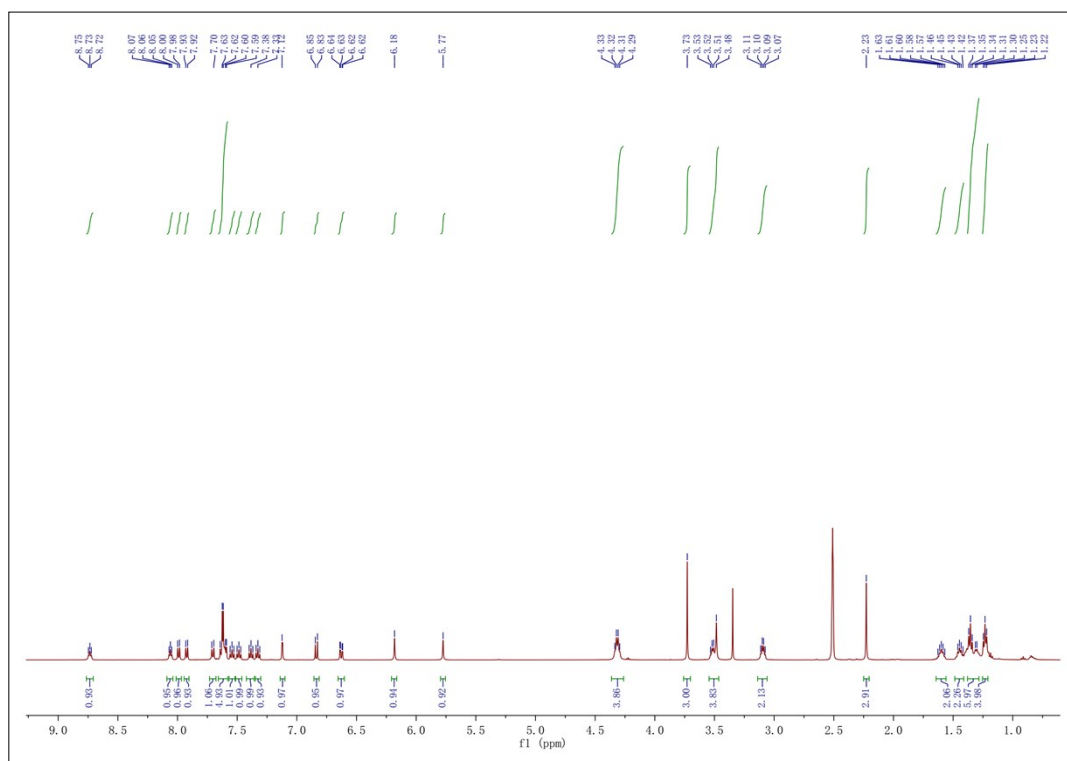


Fig. S13. ^1H NMR spectrum of IMC-DAH-SQ in $\text{DMSO-}d_6$ solvent.

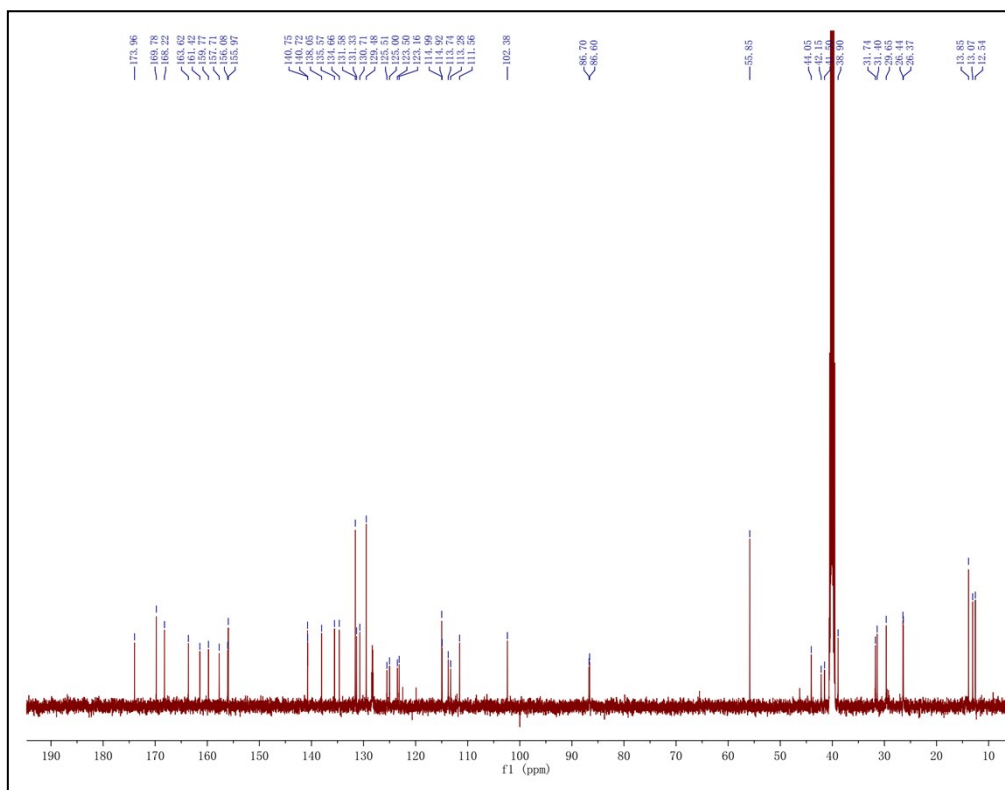


Fig. S14. ^{13}C NMR spectrum of IMC-DAH-SQ in $\text{DMSO-}d_6$ solvent.

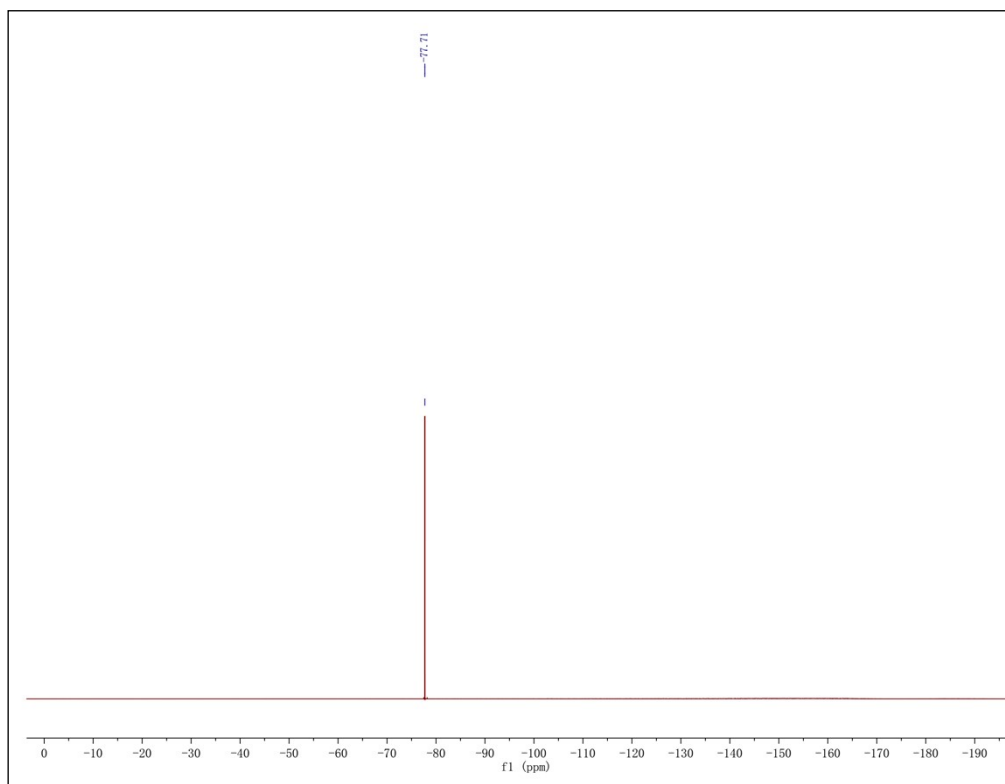


Fig. S15. ^{19}F NMR spectrum of IMC-DAH-SQ in $\text{DMSO-}d_6$ solvent.

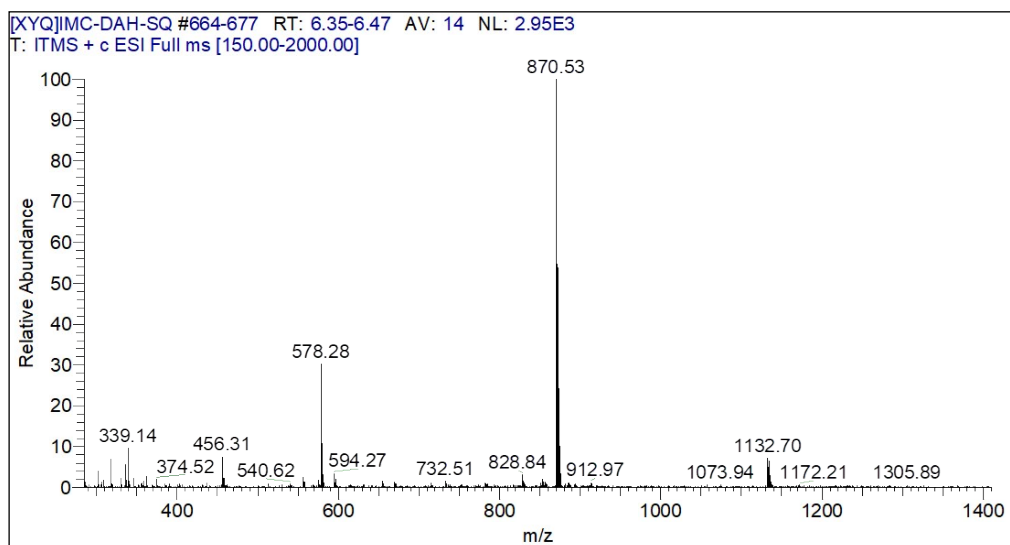


Fig. S16. ESI mass spectrum of IMC-DAH-SQ.

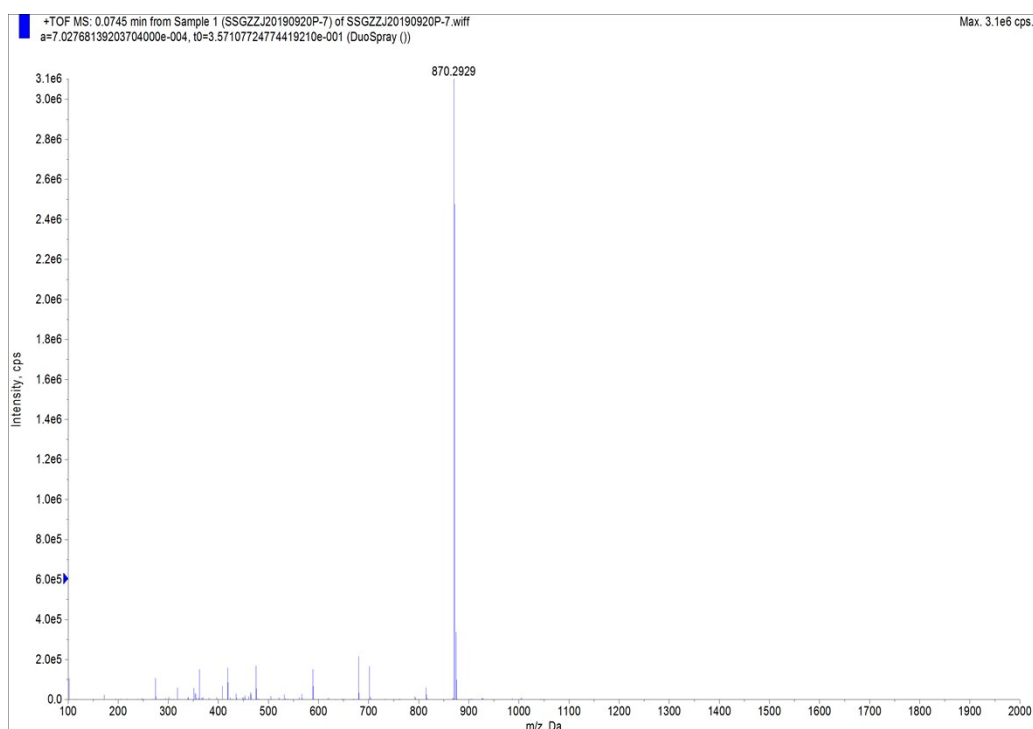


Fig. S17. TOF mass spectrum of IMC-DAH-SQ.